Appl Petrochem Res (2015) 5:9–17
DOI 10.1007/s13203-014-0046-1

ORIGINAL ARTICLE

Characterization of single-chain polymer folding using size exclusion chromatography with multiple modes of detection

Peter Frank · Alka Prasher · Bryan Tuten · Danming Chao · Erik Berda

Received: 13 January 2014 / Accepted: 27 January 2014 / Published online: 26 February 2014

Abstract We highlight here recent work from our laboratory on the subject of fabricating nanostructures from single polymer chains. These so-called single-chain nanoparticles are synthesized by inducing intra-molecular cross-linking on discrete macromolecules in dilute solution. Among the biggest challenges in this rapidly expanding area of research is reliable and accurate means to characterize this process. In this paper, we review our preferred method of characterization: size exclusion chromatography featuring multiple modes of detection. Multi-angle light scattering in conjunction with a concentration detector can provide absolute molecular weight data; viscometric detection can provide information about solution size and conformation. Correlation of these data provides a simple and robust way to quantify the process by which we fold single polymer coils into architecturally defined unimolecular nanostructures.

Keywords Single-chain nanoparticles · Polymer folding · TEM · SEC

P. Frank · A. Prasher · E. Berda (✉)
Department of Chemistry, University of New Hampshire, Durham, USA
e-mail: Erik.Berda@unh.edu

B. Tuten · E. Berda
Materials Science Program, University of New Hampshire, Durham, USA

D. Chao
Alan G. MacDiarmid Institute, College of Chemistry, Jilin University, Changchun, People's Republic of China

Introduction

A fast growing research area, single-chain nanoparticles (SCNP) have demonstrated promise for use in catalysis [1], nanoreactors [2], controlled release [3], chemical sensors [4], enzyme mimetics [5–7], diagnostics [8] and optics [9]. This breadth of application is attributed to the precise control over the composition, functionality, geometry and topology this technology permits for accessing architectures in the sub-20 nm size regime. These features are programmed into SCNP a priori by means of robust living polymerization techniques including ring-opening metathesis polymerization [10] (ROMP), reversible addition-fragmentation chain-transfer [11] (RAFT), and atom transfer radical polymerization [12] (ATRP). Such techniques afford parent polymers with narrow molecular weight distributions ($Đ$), targeted molecular weights, tunable functionality and diverse architectures [13–17]. These parent chains are then subjected to intra-molecular cross-linking under ultra-dilute conditions, thus folding the chains into architecturally defined nanoparticles with dimensions smaller than the original dimensions of the solvated coil (Fig. 1) [18].

Although young, this field is developing rapidly; a number of important contributions have appeared in the recent literature. [1, 12, 19–21] The Meijer group showed that the molecular weight and backbone rigidity of the parent polymer does not significantly influence the SCNP fabrication induced by supramolecular interactions. Instead, the solvent plays a key role in mediating intra-molecular folding [21]. Meijer and coworkers also expanded the scope of possible architectures by successfully synthesizing SCNP from cylindrical brush block polymers as well as an orthogonally collapsible ABA triblock copolymer [6, 22]. Additionally, this group studied

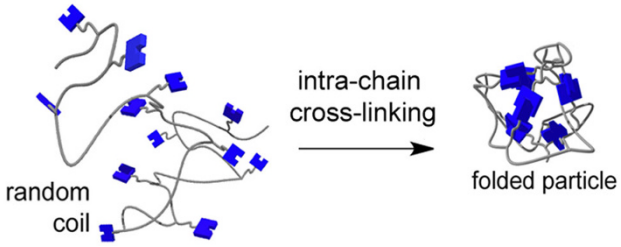

Fig. 1 Schematic representation of SCNP synthesis

temperature and co-solvent induced changes in the secondary structures of benzene-1,3,5-tricarboxamides (BTA)-based SCNPs, and developed a compartmentalized metal ion SCNP sensor that shows impressive binding affinities [4, 23]. The Barner-Kowollik group demonstrated a photo-induced Diels–Alder ligation to create SCNP in addition to using metal–ligand complexation to induce controlled folding by linking chain ends [1, 24]. Other work has demonstrated that SCNP can be formed from a host of reactions including benzocylcobutene coupling [25], olefin cross-metathesis [26], azide–alkyne click chemistry [19, 27–30], thiol-ene click chemistry [31, 32], Bergman cyclization [33–35], Curtius rearrangement [36], Glasser–Hay coupling [37], nitrene-mediated C-alkylation (sulfonyl azide) [38], oxidative polymerization through pendant moieties [12], benzosulfone chemistry [39], carbodiimide coupling [40], benzoxazine chemistry [11], amide bond formation [10, 31], cinnamoyl [40] and coumarin [2] photodimerization, guest–host interactions [41], hydrogen bonding [20, 42–44], and vulcanization [45].

These methods draw synthetic parallel to nature's elegant biomacromolecules, albeit in a crude and simplistic fashion [3, 5]. Given that synthetic polymers are always subject to distributions in molecular weights and heterogeneities in microstructure [46, 47], it is important to develop convenient and consistent methods for characterizing SCNP fabrication. We discuss here the analysis of SCNPs using size exclusion chromatography (SEC), specifically the application of multi-detection SEC. We have recently shown that when applied in conjunction with microscopy and dynamic light scattering (DLS), multi-detection SEC is a powerful tool for studying the folding of individual polymer chains into architectural defined nanostructures.

Polymer design and SCNP synthesis

There are a variety of synthetics strategies that can be used to fabricate SCNP [48]. The first methodology successfully employed in our labs involves the addition of an external, bifunctional cross-linker to a chain decorated with complementary reactive handles (Scheme 1) [10]. Polymer chains decorated with cyclic anhydride units were folded by the introduction of *p*-aminophenyl disulfide as the bifunctional cross-linker. We chose to work with poly(norbornene-exo-anhydride), as the requisite reactive monomer is commercially available and polymerization (or copolymerization with cyclooctene) via ROMP proceeds rapidly with excellent control. In series **1a**, the number of intra-chain linkages can be controlled by modulating the amount of bifunctional diamine cross-linker added to a solution of

Scheme 1 Synthetic approach to series **1** via addition of an external bifunctional cross-linker

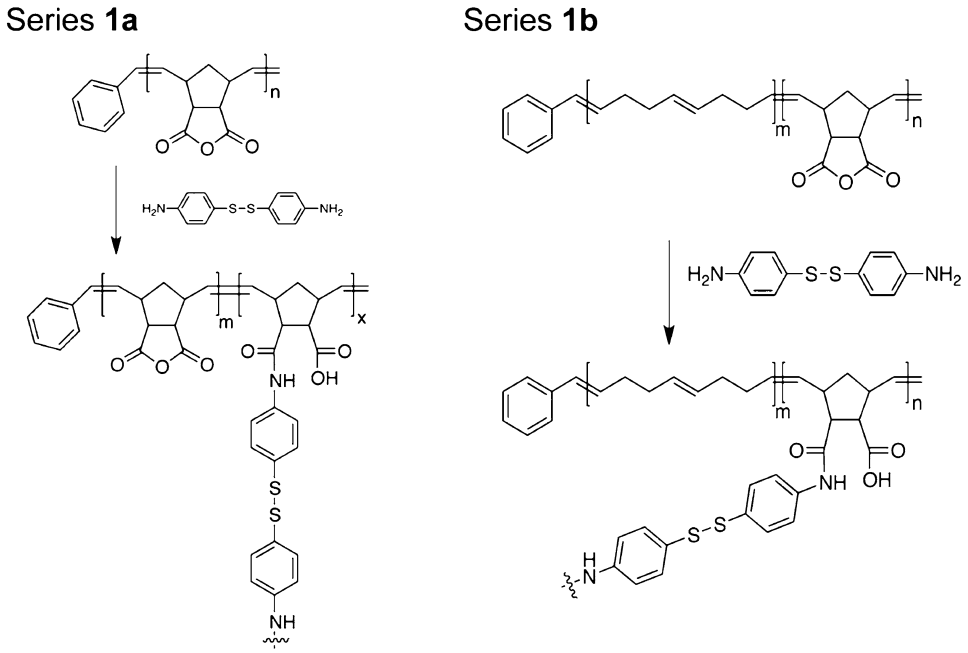

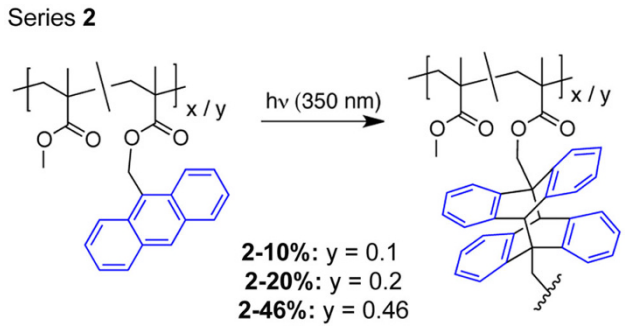

Scheme 2 Synthetic approach to series **2** using photo cross-linkable pendant groups

the polyanhydride. In series **1b**, the extent of intra-chain cross-links is controlled by changing the feed ratio of anhydride co-monomer relative to cyclooctene, followed by the addition of stoichiometric amounts of diamine. Using a cross-linker with a reversible covalent bond permits the unfolding and refolding of the chain and allows us to better characterize this coil to globule transition [10].

The second route we are using to fabricate SCNPs involves the homocoupling of a built in functional unit [49]. For series **2**, foldable methacrylic chains bearing pendant anthracene units were synthesized by RAFT polymerization (Scheme 2). Anthracene is well known for its ability to undergo a photo-

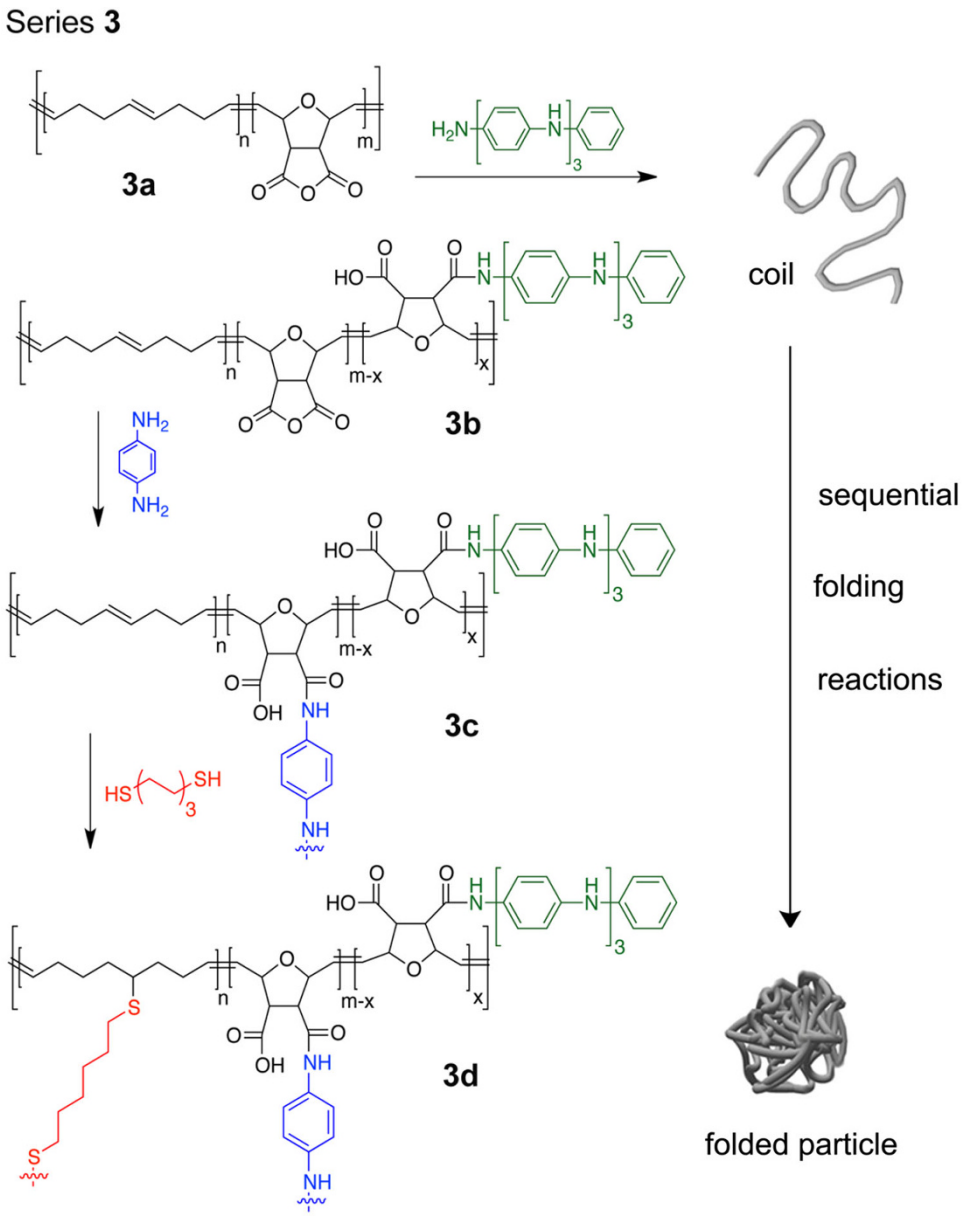

Scheme 3 Synthetic approach to series **3** using sequentially activated orthogonal intra-chain interactions

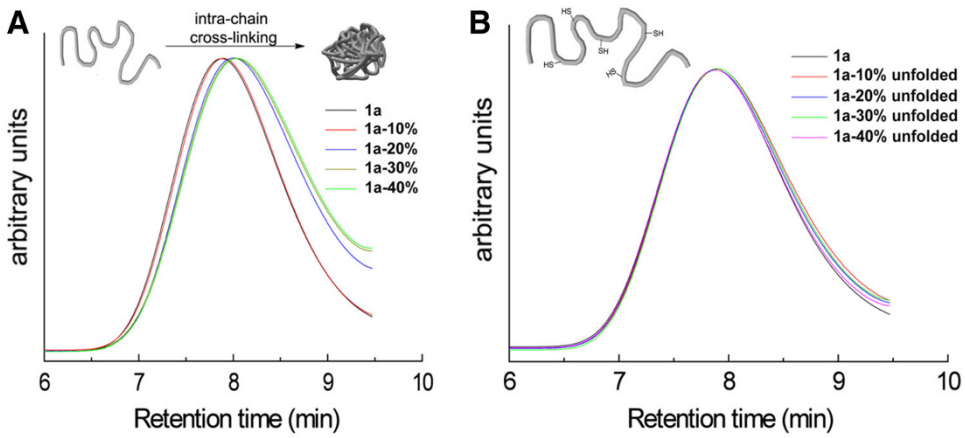

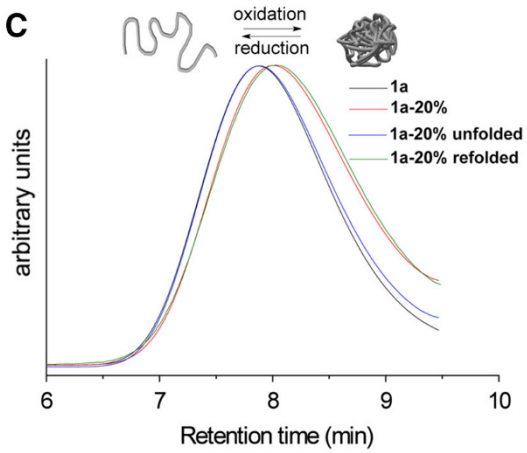

Fig. 2 SEC traces for series **1a**. **a** Addition of varying amounts of cross-linker, **b** after unfolding via disulfide reduction, **c** reversible folding and unfolding via redox chemistry (Tuten et al. [10]—adapted with permission of The Royal Society of Chemistry)

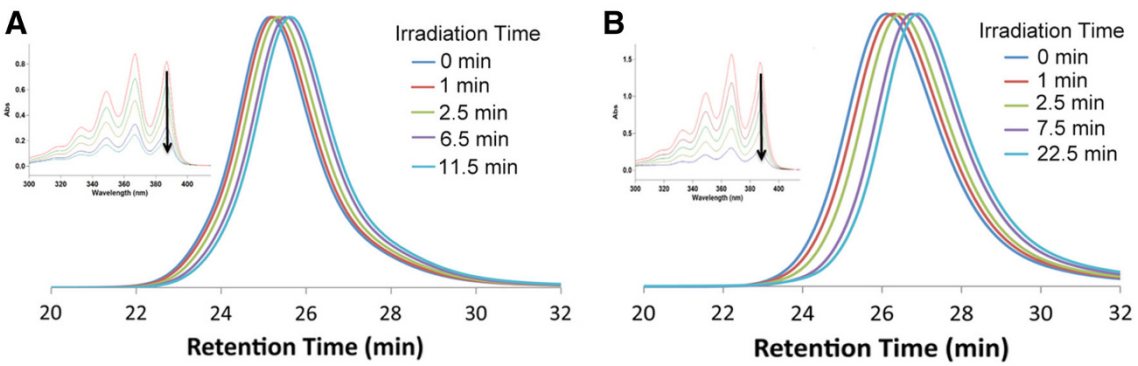

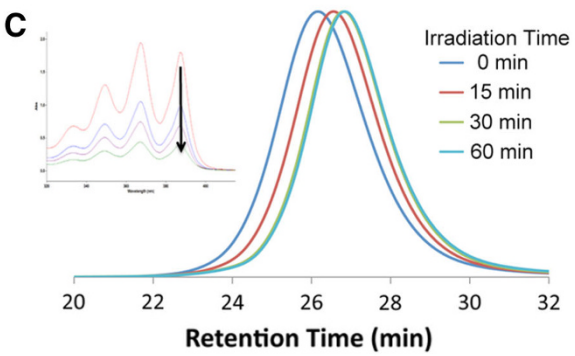

Fig. 3 SEC traces and corresponding UV–Vis spectra for series **2** photodimerization studies (Frank et al. [49]—adapted with permission of John Wiley And Sons Inc)

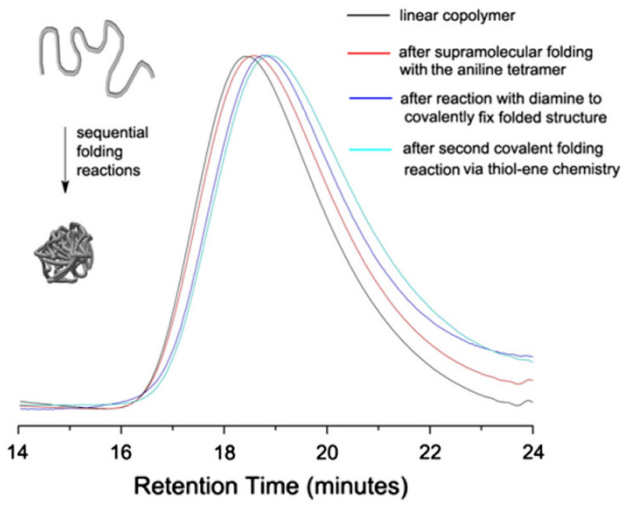

Fig. 4 SEC traces displaying the decrease in hydrodynamic volume with each sequential folding reaction for series 3 (Chao et al. [31]—adapted with permission of The Royal Society of Chemistry)

Table 1 SEC data for series **1b**

	Peak retention time (min)[a]	M_w (kg/mol)[b]	$Đ$	$[\eta]$ (mL/g)	R_h (nm)
Parent polymer (**1b**)	17.8	50.1	1.22	13.9	4.5
Folded nanoparticle	18.8	59.3	1.32	8.7	3.9

[a] Retention times are from MALS detector trace

[b] Absolute molecule weight calcultated by MALS

Table 2 SEC data for series **2** before and after complete photo-induced folding

Polymer	Irradiation time (min)	Peak retention time (min)	M_w (kg/mol)	$Đ$	R_h (nm)	$[\eta]$
2a-10	0	24.9	30.8	1.17	4	13.3
	11.5	25.4	33.5	1.16	3.4	7.5
2b-20	0	25.6	30.6	1.14	3.6	9.5
	22.5	26.5	29.9	1.14	2.9	5.1
2c-46	0	25.7	42.9	1.16	3.5	6.6
	60	26.4	36.7	1.14	2.3	2.4

Table 3 Comparison of predicted vs. actual absolute M_w for series **3**

Polymer	Predicted molecular weights M_w (kg/mol)	Actual molecular weights M_w (kg/mol)	R_h (nm)
3a	16.1	15.0	6.5
3b	19.7	19.9	5.7
3c	20.5	22.6	4.9
3d	23.9	23.3	4.3

R_h values from DLS confirm the efficacy of each sequential folding reaction

induced 4 + 4 cycloaddition when irradiated with 350 nm-centered UV light, resulting in photodimers that can be reversed via irradiation with wavelengths <300 nm or thermally at temperatures >180 °C [50], providing an attractive route to synthesizing thermally responsive and photosensitive nanomaterials. In addition, using light as stimulus for SCNP fabrication offers additional functional group tolerance that other cross-linking strategies lack [49].

A third method for SCNP fabrication takes advantage of multiple orthogonal chemistries triggered sequentially to fold synthetic chains into particles [31]. Scheme 3 shows a series of poly(oxanorbornene anhydride-*co*-cyclooctadiene) materials synthesized using ROMP. Analogous to series **1**, the polymer structures contained in series **3** feature anhydride groups as reactive handles that can be easily modified with a variety of nucleophiles, simultaneously inducing folding and installing functionality. In this system, aniline tetramer (AT) was used to fold the chains via supramolecular interactions (π–π and hydrogen bonding) between these pendant groups. The chains were then reacted with *p*-aminoaniline, a bifunctional covalent cross-linker that pulls in the remaining anhydride units and further collapses the chain. Finally, internal olefin units installed within the backbones during ROMP were connected using photoinitiated thiol-ene click chemistry with 1,6-hexanedithiol as a bifunctional cross-linker. This sequential folding approach demonstrates that the application of orthogonal chemistries in a synergistic fashion results in more tightly collapsed structures with the goal of more closely mimicking natural folded polymeric constructs. [31]

SCNP characterization

Conventional SEC

SEC with conventional calibration is the standard method used to characterize SCNPs formation. Comparing the retention time of the parent polymer chains to the retention time of the folded nanoparticles after intramolecular cross-linking is induced typically reveals shifts to longer retention times. This indicates a decrease in hydrodynamic volume based on the inherent principles of size exclusion chromatography [51–53]. This is clearly demonstrated in all of the polymer series discussed here [10, 31, 49].

SEC traces for series **1a** below show the effect of adding increasing amounts of bifunctional cross-linker: as more intra-chain linkages are formed the SEC traces shift to longer retention times as expected (Fig. 2a). To ensure this is truly an effect of conformational changes and not due to other factors, such as interactions between the SEC columns and the analyte, we take advantage of the cleavable

disulfide linkage that was installed during single-chain nanoparticles formation. Cleaving this linkage after the initial folding reaction takes place allows us to determine that the shifts in the retention time is actually due to the folding of the chain and not other behavior that might affect retention time. This is indeed the case, as shown in Fig. 2b. The reduction of the disulfide bridges via dithiothreitol (DTT) results in the unfolding of the SCNPs, confirmed by SEC traces showing that retention times (and therefore hydrodynamic volume) revert to those of the parent polymer chain, regardless of the amount of cross-linker added. Furthermore, refolding of the unfolded chains via thiol oxidation in the presence of catalytic $FeCl_3$ revealed shifts to longer retention times, indicating the reduction in the solvent dynamic volume (refolding), confirming the utility of this characterization method as well as demonstrating this chemistry as a route to responsive nanostructures (Fig. 2c).

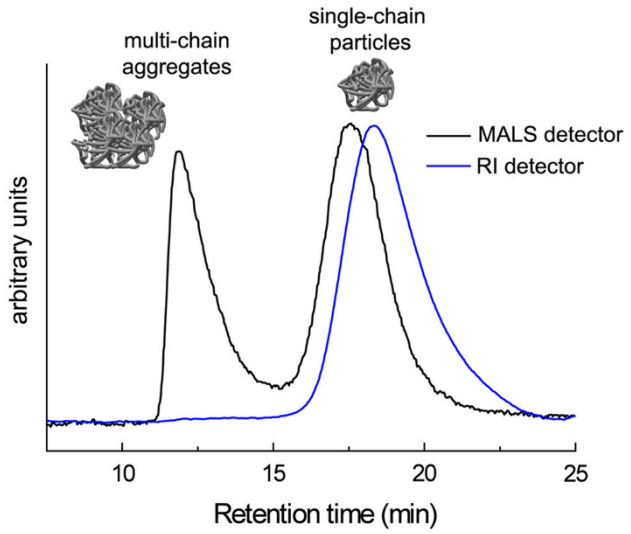

Fig. 5 MALS and RI detection traces for SEC of **1b** highlighting the ability of MALS to detect large, multi-chain aggregates (Tuten et al. [10]—Reproduced by permission of The Royal Society of Chemistry)

Analyzing the SEC traces from series **2** shows that the extent of intra-molecular folding or collapse can be controlled very easily using built-in reactive co-monomer. Both reaction time and the amount of co-monomer incorporation can be used to control the extent of intra-chain cross-links when employing this method. Figure 3a–c highlights this behavior. All samples show steady shifts to longer retention times with increasing irradiation times, an

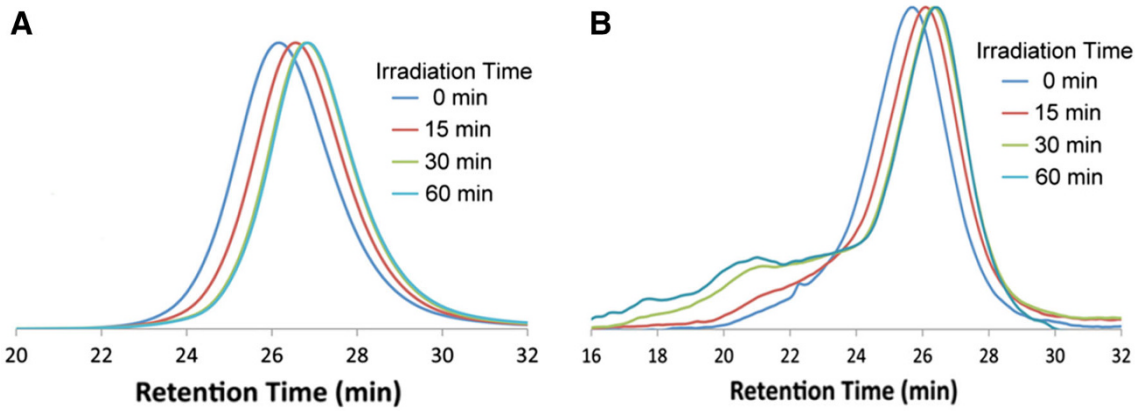

Fig. 6 SEC traces for **2c-46** photodimerization studies showing the appearance of multi-chain aggregates. **a** UV detector traces, **b** MALS detector traces (Frank et al. [49]—Reproduced by permission of John Wiley And Sons Inc)

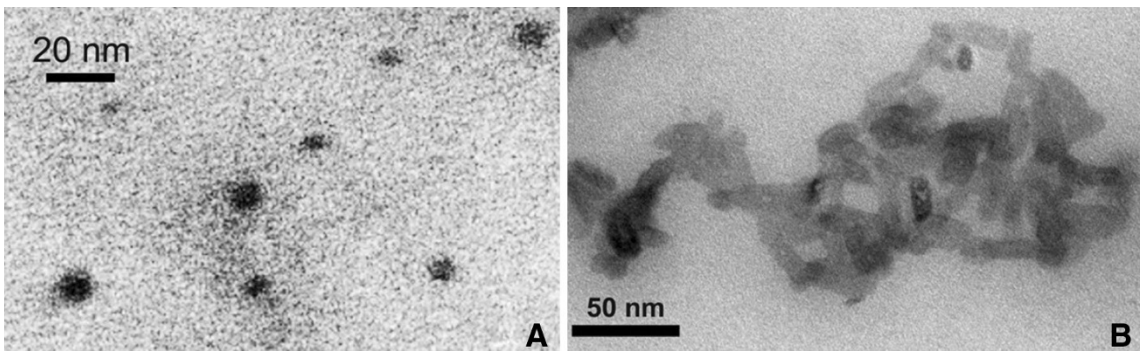

Fig. 7 TEM images of SCNP obtained from **1b** (**a**) and **2a-10** (**b**)

indication that folding is occurring with the formation of anthracene photodimers. Anthracene dimerization was confirmed by the disappearance of the characteristic anthracene absorption peak in the UV–Vis spectra (insets in Fig. 3). The effect of reactive co-monomer incorporation is clearly observed here: samples with 10 % (**2a-10**) anthracene co-monomer showed the least pronounced changes in retention time when compared to the samples with 20 % (**2a-20**) and 46 % (**2a-46**) anthracene co-monomer (Fig. 3).

Conventional SEC reveals the same behavior even when multiple orthogonal intra-chain cross-linking chemistries are used. Figure 4 shows that for polymers in series **3**, the expected shifts in retention time confirm the efficacy of each folding reaction when engaged sequentially. As expected, the SEC trace of the final nanoparticle shifted to the longest retention time indicating a more tightly wrapped structure consistent with theory and experiment [6].

Triple detection SEC

The application of standard SEC as described above provides useful qualitative information about changes in the solution conformation of polymer chains during SCNP fabrication. Still this method is not without ambiguities, especially with regards to actual changes in molecular weight (or lack thereof) when triggering intra-chain cross-linking. Since relative molecular weight and retention time are linked in traditional SEC, it is impossible to formally characterize SCNP molecular weight with this technique. Furthermore, while shifts in retention time certainly signify changes in hydrodynamic volume it is impossible to quantify these changes with standard SEC measurements alone. Dynamic light scattering (DLS) in conjunction with SEC can be a very useful tool for SCNP characterization, but lacks the chromatographic separation provided by SEC.

To alleviate some of these issues our group implemented SEC with multiple modes of detection for SCNP characterization. The use of multi-angle light scattering (MALS) detection with SEC allows the determination of polymer and SCNP molecular weight independent of retention time [54]. The addition of an inline differential viscometer permits characterization of molecular conformation, including hydrodynamic radius, for each thin chromatographic slice as the sample elutes from the SEC column. With this setup, the absolute molecular weight of the parent polymers can be easily measured and used to calculate the expected SCNP molecular weight. Comparing this value with the experimental absolute SCNP molecular weight can provide useful quantitative information about the chemistry involved in this process. Changes in retention time, which are assumed to correlate with changes in solvated volume, can likewise be readily quantified by this method. Recent work from our lab demonstrating the utility of this technique is highlighted below.

Table 1 summarizes the triple detection data for series **1b.** As expected, the MALS detector trace shows a shift to longer retention time after addition of cross-linker similar to what we observed using standard SEC. Examining the absolute molecular weight reveals that although the SCNP curve shifted to a longer retention time the molecular weight actually increased by the amount predicted with the addition of stoichiometric cross-linker. In addition, the viscometric data confirm and quantify the decrease in hydrodynamic radius. It further reveals a decrease in intrinsic viscosity after SCNP formation consistent with theory and experiment [55].

The SEC data for series **2** showed similar behavior where shifts to longer retention times occur after folding as expected. The viscometric data reveals a decrease in both intrinsic viscosity and hydrodynamic radius. The absolute molecular weight, predicted to remain constant, changes only slightly and is consistent with a primarily unimolecular phenomenon (Table 2). This series also displays the trend, although unsurprising, that the extent of reactive co-monomer incorporation directly dictates how much folding will occur.

SEC MALS data from series **3**, shown in Table 3, again highlight how useful this technique can be as a quantitative tool. For these polymers, the comparison between the predicted and the measured absolute molecular weights demonstrates that the folding chemistry proceeded as designed. In addition, DLS measurements confirmed that retention time shifts witnessed in SEC measurements (Table 3) are indeed due to folding.

Intra-chain versus inter-chain reactions

A crucial bit of qualitative data provided by SEC MALS is the distinction between intra-chain folding and inter-chain coupling. In our experience, MALS is capable of detecting larger nanoaggregates in very minute concentrations while traditional SEC detectors such as UV and RI do not show the characteristic aggregate peak [10, 49]. For series **1**, multi-chain aggregates were detectable via MALS while virtually unseen in RI traces (Fig. 5) [10].

Likewise for series **2**, the UV detector fails to detect inter-chain aggregates that are readily observed by MALS, evident in the emergence of peak shoulders in MALS traces. These data also suggest that at a certain level of reactive co-monomer incorporation inter-chain coupling becomes unavoidable (Fig. 6) [49]. Thus, triple detection SEC provides a robust method for analyzing polymer folding chemistry and confirming single-chain behavior.

Correlating solution measurements with other characterization tools

We highlighted in the previous sections how triple detection SEC can be applied to effectively characterize single-chain folding. Additional secondary characterization techniques can offer invaluable information about SCNP size and shape, including small angle neutron scattering (SANS) [3, 23], thorough DLS measurements [4, 23], atomic force microscopy (AFM) [11, 19, 20, 26, 29, 30, 33, 39, 42, 43, 56, 57], and transmission electron microscopy (TEM) [2, 7, 10, 11, 27, 38, 49]. We found TEM particularly useful as a tool to provide visual evidence for SCNP formation. Figure 7 shows representative images from series **1** (**1b**) and series **2** (**2a-10**). In each case, the images reveal nanostructures with dimensions on the same order of magnitude as numbers obtained from solution measurements. Interestingly, series **2** SCNP adopt an oblong ellipsoid geometry, rather than a spherical conformation. We are still investigating the cause of this behavior, which is consistent with form factor measurements made by others [3, 23].

Summary

In summary, conventionally calibrated SEC is a satisfactory method to characterize SCNP via interpretation of comparative shifts in retention time. Evolving this tool by marrying SEC with MALS and viscometric detection affords a precise and reliable method for the qualitative and quantitative study of SCNP fabrication. This methodology facilitates the detailed investigation of structure property relationships using absolute molecular weight, intrinsic viscosity, and hydrodynamic radius of SCNP systems. During SCNP formation, the decrease in both the intrinsic viscosity and hydrodynamic radius is observed with, or in the absence of, concurrent changes in the absolute molecular weight depending on the folding technique employed. Triple detection SEC in conjunction with additional characterization tools including TEM and DLS provides a variety of useful information for studying the fascinating and rapidly expanding research area of single-chain folding processes and single-chain nanoparticles.

References

1. Willenbacher J, Altintas O, Roesky PW, Barner-Kowollik C (2013) Macromol Rapid Commun 1521–3927
2. He J, Tremblay L, Lacelle S, Zhao Y (2011) Preparation of polymer single chain nanoparticles using intramolecular photodimerization of coumarin. Soft Matter 7:2380–2386
3. Sanchez-Sanchez A, Akbari S, Etxeberria A, Arbe A, Gasser U, Moreno AJ, Colmenero J, Pomposo JA (2013) "Michael" nanocarriers mimicking transient-binding disordered proteins. ACS Macro Lett 2:491–495
4. Gillissen MAJ, Voets IK, Meijer EW, Palmans ARA (2012) Single chain polymeric nanoparticles as compartmentalised sensors for metal ions. Polym Chem 3:3166–3174
5. Perez-Baena I, Barroso-Bujans F, Gasser U, Arbe A, Moreno AJ, Colmenero J, Pomposo JA (2013) Endowing single-chain polymer nanoparticles with enzyme-mimetic activity. ACS Macro Lett 2:775–779
6. Hosono N, Gillissen MAJ, Li Y, Sheiko SS, Palmans ARA, Meijer EW (2013) Orthogonal self-assembly in folding block copolymers. J Am Chem Soc 135:501–510
7. Terashima T, Mes T, De Greef TFA, Gillissen MAJ, Besenius P, Palmans ARA, Meijer EW (2011) Single-chain folding of polymers for catalytic systems in water. J Am Chem Soc 133:4742–4745
8. Murray BS, Fulton DA (2011) Dynamic covalent single-chain polymer nanoparticles. Macromolecules 44:7242–7252
9. Wang Y, Dong L, Xiong R, Hu AJ (2013) Practical access to bandgap-like N-doped carbon dots with dual emission unzipped from PAN@PMMA core–shell nanoparticles. Mater Chem C 1:7731–7735
10. Tuten BT, Chao D, Lyon CK, Berda EB (2012) Single-chain polymer nanoparticles via reversible disulfide bridges. Polym Chem 3:3068–3071. doi:10.1039/c2py20308a
11. Wang P, Pu H, Jin MJ (2011) Single-chain nanoparticles with well-defined structure via intramolecular crosslinking of linear polymers with pendant benzoxazine groups. Polym Sci Part A Polym Chem 49:5133–5141
12. Dirlam PT, Kim HJ, Arrington KJ, Chung WJ, Sahoo R, Hill LJ, Costanzo PJ, Theato P, Char K, Pyun J, Kim J, Chung J (2013) Single chain polymer nanoparticles via sequential ATRP and oxidative polymerization. Polym Chem 4:3765–3773
13. Moad G, Chong YK, Postma A, Rizzardo E, Thang SH (2005) Advances in RAFT polymerization: the synthesis of polymers with defined end-groups. Polymer 46:8458–8468
14. Moad G, Rizzardo E, Thang SH (2005) Living radical polymerization by the RAFT process. Aust J Chem 58:379–410
15. Alfred SF, Lienkamp K, Madkour AE, Tew GN (2008) Water-soluble ROMP polymers from amine-functionalized norbornenes. Polymer 6672–6676
16. Bielawski CW, Grubbs RH (2007) Living ring-opening metathesis polymerization. Prog Polym Sci 32:1–29
17. Matyjaszewski K, Tsarevsky NV (2009) Nanostructured functional materials prepared by atom transfer radical polymerization. Nat Chem 1:276–288
18. Altintas O, Barner-Kowollik C (2012) Single chain folding of synthetic polymers by covalent and non-covalent interactions: current status and future perspectives. Macromol Rapid Commun 33:958–971
19. Ormategui N, García I, Padro D, Cabañero G, Grande HJ, Loinaz I (2012) Synthesis of single chain thermoresponsive polymer nanoparticles. Soft Matter 8:734–740
20. Foster EJ, Berda EB, Meijer EW (2009) Metastable supramolecular polymer nanoparticles via intramolecular collapse of single polymer chains. J Am Chem Soc 131:6964–6966
21. Stals PJM, Gillissen MAJ, Nicolaÿ R, Palmans ARA, Meijer EW (2013) The balance between intramolecular hydrogen bonding, polymer solubility and rigidity in single-chain polymeric nanoparticles. Polym Chem 4:2584–2597

22. Stals PJM, Li Y, Burdyńska J, Nicolaÿ R, Nese A, Palmans ARA, Meijer EW, Matyjaszewski K, Sheiko SS (2013) How far can we push polymer architectures? J Am Chem Soc 135:11421–11424
23. Gillissen MAJ, Terashima T, Meijer EW, Palmans ARA, Voets IK (2013) Sticky supramolecular grafts stretch single polymer chains. Macromolecules 46:4120–4125
24. Altintas O, Willenbacher J, Wuest KNR, Oehlenschlaeger KK, Krolla-Sidenstein P, Gliemann H, Barner-Kowollik C (2013) A mild and efficient approach to functional single-chain polymeric nanoparticles via photoinduced Diels–Alder ligation. Macromolecules 46:8092–8101
25. Harth E, Van Horn B, Lee VY, Germack DS, Gonzales CP, Miller RD, Hawker CJ (2002) A facile approach to architecturally defined nanoparticles via intramolecular chain collapse. J Am Chem Soc 124:8653–8660
26. Cherian AE, Sun FC, Sheiko SS, Coates GW (2007) Formation of nanoparticles by intramolecular cross-linking: following the reaction progress of single polymer chains by atomic force microscopy. J Am Chem Soc 129:11350–11351
27. De Luzuriaga AR, Ormategui N, Grande HJ, Odriozola I, Pomposo JA, Loinaz I (2008) Intramolecular click cycloaddition: an efficient room-temperature route towards bioconjugable polymeric nanoparticles. Macromol Rapid Commun 29:1156–1160
28. Schmidt BVKJ, Fechler N, Falkenhagen J, Lutz J-F (2011) Controlled folding of synthetic polymer chains through the formation of positionable covalent bridges. Nat Chem 3:234–238
29. Perez-Baena I, Loinaz I, Padro D, García I, Grande HJ, Odriozola I (2010) Single-chain polyacrylic nanoparticles with multiple Gd(iii) centres as potential MRI contrast agents. J Mater Chem 20:6916–6922
30. Oria L, Aguado R, Pomposo JA, Colmenero J (2010) A versatile "click" chemistry precursor of functional polystyrene nanoparticles. Adv Mater 22:3038–3041
31. Chao D, Jia X, Tuten B, Wang C, Berda EB (2013) Controlled folding of a novel electroactive polyolefin via multiple sequential orthogonal intra-chain interactions. Chem Commun 49:4178–4180. doi:10.1039/c2cc37157j
32. Ding L, Yang G, Xie M, Gao D, Yu J, Zhang Y (2012) More insight into tandem ROMP and ADMET polymerization for yielding reactive long-chain highly branched polymers and their transformation to functional polymer nanoparticles. Polymer 53:333–341
33. Zhu B, Ma J, Li Z, Hou J, Cheng X, Qian G, Liu P, Hu A (2011) Formation of polymeric nanoparticles via Bergman cyclization mediated intramolecular chain collapse. J Mater Chem 21:2679–2683
34. Zhu B, Sun S, Wang Y, Deng S, Qian G, Wang M, Hu AJ (2013) Preparation of carbon nanodots from single chain polymeric nanoparticles and theoretical investigation of the photoluminescence mechanism. Mater Chem C 1:580–586
35. Zhu B, Qian G, Xiao Y, Deng S, Wang M, Hu AJ (2011) A convergence of photo-bergman cyclization and intramolecular chain collapse towards polymeric nanoparticles. Polym Sci Part A Polym Chem 49:5330–5338
36. Zheng H, Ye X, Wang H, Yan L, Bai R, Hu W (2011) A facile one-pot strategy for preparation of small polymer nanoparticles by self-crosslinking of amphiphilic block copolymers containing acyl azide groups in aqueous media. Soft Matter 7:3956–3962
37. Sanchez-Sanchez A, Asenjo-Sanz I, Buruaga L, Pomposo JA (2012) Naked and self-clickable propargylic-decorated single-chain nanoparticle precursors via redox-initiated RAFT polymerization. Macromol Rapid Commun 33:1262–1267
38. Jiang X, Pu H, Wang P (2011) Polymer nanoparticles via intramolecular crosslinking of sulfonyl azide functionalized polymers. Polymer 52:3597–3602
39. Adkins CT, Muchalski H, Harth E (2009) Nanoparticles with individual site-isolated semiconducting polymers from intramolecular chain collapse processes. Macromolecules 42:5786–5792
40. Njikang G, Liu G, Curda SA (2008) Tadpoles from the intramolecular photo-cross-linking of Diblock copolymers. Macromolecules 41:5697–5702
41. Appel EA, Dyson J, del Barrio J, Walsh Z, Scherman OA (2012) Formation of single-chain polymer nanoparticles in water through host-guest interactions. Angew Chem Int Ed Engl 51:4185–4189
42. Foster EJ, Berda EB, Meijer EWJ (2011) Tuning the size of supramolecular single-chain polymer nanoparticles. Polym Sci Part A Polym Chem 49:118–126
43. Berda EB, Foster EJ, Meijer EW (2010) Toward controlling folding in synthetic polymers: fabricating and characterizing supramolecular single-chain nanoparticles. Macromolecules 43:1430–1437
44. Seo M, Beck BJ, Paulusse JMJ, Hawker CJ, Kim SY (2008) Polymeric nanoparticles via noncovalent cross-linking of linear chains. Macromolecules 41:6413–6418
45. Cheng C, Qi K, Germack DS, Khoshdel E, Wooley KL (2007) Synthesis of core-crosslinked nanoparticles with controlled cylindrical shape and narrowly-dispersed size via core-shell brush block copolymer templates. Adv Mater 19:2830–2835
46. Berda EB, Baughman TW, Wagener KBJ (2006) Precision branching in ethylene copolymers: Synthesis and thermal behavior. Polym Sci Part A Polym Chem 44:4981–4989
47. Odian G (2004) Principles of polymerization, 4th edn. Wiley, New Jersey, p 832
48. Aiertza MK, Odriozola I, Cabañero G, Grande H-J, Loinaz I (2012) Single-chain polymer nanoparticles. Cell Mol Life Sci 69:337–346
49. Frank PG, Tuten BT, Prasher A, Chao D, Berda EB (2014) Intrachain photodimerization of pendant anthracene units as an efficient route to single-chain nanoparticle fabrication. Macromol Rapid Commun 35:249–253. doi:10.1002/marc.201300677
50. Becker HD (1993) Unimolecular photochemistry of anthracenes. Chem Rev 93:145–172
51. Sun T, Chance RR, Graessley WW, Lohse DJ (2004) A study of the separation principle in size exclusion chromatography. Macromolecules 37:4304–4312
52. Grubisic Z, Rempp P, Benoit HJ (1967) A universal calibration for gel permeation chromatography. Polym Sci Part B Polym Lett 5:753–759
53. Moore JCJ (1964) Gel permeation chromatography. I. A new method for molecular weight distribution of high polymers. Polym Sci Part A Gen Pap 2:835–843
54. Wyatt PJ (1993) Light scattering and the absolute characterization of macromolecules. Anal Chim Acta 272:1–40
55. Beck JB, Killops KL, Kang T, Sivanandan K, Bayles A, Mackay ME, Wooley KL, Hawker CJ (2009) Facile preparation of nanoparticles by intramolecular crosslinking of isocyanate functionalized copolymers. Macromolecules 42:5629–5635
56. Kim Y, Pyun J, Fréchet JMJ, Hawker CJ, Frank CW (2005) The dramatic effect of architecture on the self-assembly of block copolymers at interfaces. Langmuir 21:10444–10458
57. Croce TA, Hamilton SK, Chen ML, Muchalski H, Harth E (2007) Alternative o—quinodimethane cross-linking precursors for intramolecular chain collapse nanoparticles. Macromolecules 40:6028–6031